Comparative Study of Different Discrete Wavelet Based Neural Network Models for long term Drought Forecasting

Article *in* Water Resources Management · January 2023

DOI: 10.1007/s11269-023-03432-0

CITATIONS
7

READS
281

7 authors, including:

Salim Djerbouai
University of Msila
11 PUBLICATIONS **132** CITATIONS
SEE PROFILE

Souag-Gamane Doudja
University of Science and Technology Houari Boumediene
27 PUBLICATIONS **1,138** CITATIONS
SEE PROFILE

Ferhati Ahmed
university of M'sila
16 PUBLICATIONS **60** CITATIONS
SEE PROFILE

Omar Djoukbala
University of Sidi-Bel-Abbes
14 PUBLICATIONS **193** CITATIONS
SEE PROFILE

Water Resources Management
https://doi.org/10.1007/s11269-023-03432-0

Comparative Study of Different Discrete Wavelet Based Neural Network Models for long term Drought Forecasting

Djerbouai Salim[1] · Souag-Gamane Doudja[2] · Ferhati Ahmed[1] · Djoukbala Omar[1] · Dougha Mostafa[1] · Benselama Oussama[1] · Hasbaia Mahmoud[1]

Received: 4 November 2022 / Accepted: 15 January 2023

Abstract
Recently, coupled Wavelet transform and Neural Networks models (WANN) were extensively used in hydrological drought forecasting, which is an important task in drought risk management. Wavelet transforms make forecasting model more accurate, by extracting information from several levels of resolution. The selection of an adequate mother wavelet and optimum decomposition level play an important role for successful implementation of wavelet neural network based hydrologic forecasting models.

The main objective of this research is to look into the effects of various discrete wavelet families and the level of decomposition on the performance of WANN drought forecasting models that are developed for forecast drought in the Algerois catchment for long lead time. The Standard Precipitation Index (SPI) is used as a drought measuring parameter at three-, six- and twelve-month scales. Suggested WANN models are tested using 39 discrete mother wavelets derived from five families including Haar, Daubechies, Symlets, Coiflets and the discrete approximation of Meyer. Drought is forecasted by the best model for various lead times varying from 1-month lead time to the maximum forecast lead time. The obtained results were evaluated using three performance criteria (NSE, RMSE and MAE).

The results show that WANN models with discrete approximation of Meyer have the best forecast performance. The maximum forecast lead times are 36-month for SPI-12, 18-month for SPI-6 and 7- month for the SPI-3. Drought forecasting for long lead times have significant values in drought risk and water resources management.

Keywords Algerois catchment · Drought · Forecasting · Neural networks · SPI · Wavelet transforms

Abbreviations

✉ Djerbouai Salim
Salim.djerbouai@univ-msila.dz

[1] CEHSD laboratory, Hydraulics Department, University of M'sila, Ichebila, PO Box 166, 28000 M'sila, Algeria

[2] LEGHYD Laboratory, Civil engineering Department, University of Science and Technology Houari Boumediene, BP 32 Bab-Ezzouar, Algiers, Algeria

ANN	Artificial Neural Networks
WANN	Wavelet Artificial Neural Networks
SPI	Standard Precipitation Index
NSE	Nash-Sutcliffe Efficiency coefficient
RMSE	Root Mean Squared Error
MAE	Mean Absolute Error
ACF	Autocorrelation function
PACF	Partial autocorrelation function
WMO	The World Meteorological Organization
CWT	Continuous wavelet transform
DWT	Discrete Wavelet Transform
db	Daubechies wavelets
Sym	Symlets wavelets
Coif	Coiflets wavelets
dmey	Discrete approximation of Meyer

1 Introduction

Drought is a natural part of the climate that occurs in all types of climate regimes (Wilhite 2000). As one of the severe and frequently occurring natural hazards, drought has negative impacts on human life in many regions around the word (Roushangar et al. 2022a). Drought-related events have been increasing exponentially over the last three decades in the Mediterranean regions. Algeria, like the rest of the Mediterranean countries, has been subjected to severe and long-lasting droughts over the last two decades especially the north-western part has been affected more, which is marked by a severe precipitation deficit (Medejerab and Henia 2011).

Forecasting future dry spells is crucial for long-term water management solutions and the risk assessment of drought occurrence (Bordi and Sutera 2007). Drought forecasting is also crucial in reducing the effects on water resources (Kim and Valdés 2003).Many drought indices have been developed during the last decades for drought analysis (Tigkas et al. 2019).

The Standardised Precipitation Index (SPI) is one of the most commonly used indices in the world (Mishra et al. 2007; Tigkas et al. 2019). The World Meteorological Organization (WMO) proposed the SPI as the main meteorological drought index that countries should utilize to follow and monitor drought conditions (Hayes, 2011). The SPI is a powerful, flexible index that is simple to calculate (WMO, 2012).

Drought forecasting approaches can range from the simplest to the most advanced models. Time series stochastic models have been employed in the past (Mishra and Desai 2005; Modarres 2007; Fernández et al. 2009; Han et al. 2010, 2013; Barua et al. 2012; Belayneh et al. 2014; Djerbouai and Souag-Gamane 2016; Karthika et al. 2017; Aghelpour et al. 2021). However, time series models have a limited capabilities to represent non-linear and non-stationary time series (Kim and Valdés 2003; Mishra and Desai 2006). To get around this limitation, hydrologists had to consider different methods to forecast non-stationary and non-linear times series.

In recent decades, due to their flexibility in modelling non-linear time series artificial neural networks (ANN) have shown considerable promise in water engineering problems and hydrological modelling (e.g. Mishra and Desai 2006; Morid et al. 2007; Marj and Meijerink 2011; Belayneh and Adamowski 2012; Shirmohammadi et al. 2013; Belayneh et al. 2014; Hosseini-Moghari and Araghinejad 2015; Djerbouai and Souag-Gamane 2016; Kousari et al. 2017; Anshuka et al. 2019; Drisya et al. 2021; Roushangar et al. 2022a;). If the inputs are not pre-processed, they are incapable of dealing with non-stationary data. Wavelet-transformed time series improves model accuracy by taking into account important information at multiple resolution levels. Various researchers have examined the ability of hybrid wavelet transforms and ANN models over the last decade. (e.g. Kim and Valdès 2003; Özger et al. 2012; Belayneh and Adamowski 2012; Belayneh et al. 2014; Jalalkamali et al. 2015; Djerbouai and Souag-Gamane 2016; Prasad et al. 2017 ; Soh et al. 2018; Anshuka at al. 2019; Zhang zt al. 2020; Munir et al. 2020 ; Drisya et al. 2021; Roushangar et al. 2022b; Wang et al., 2022; Piri at al., 2022). Coupled wavelet transform with artificial intelligence (AI) models, is discussed by Nourani et al. (2014). Wavelet transformation requires a mother wavelet function to perform transformation. Furthermore, the choice of an appropriate mother wavelet is very important for hybrid wavelet-based models (Shoaib et al. 2014).

In the present work we are interested to study the effect of three important parameters concerning hybrid wavelet neural network (WANN) models for long term drought forecasting. These parameters are: (1) The appropriate mother wavelet choice; (2) vanishing moment number; and (3) the optimum level of decomposition. It should be noted that this is the first study that focuses on the effect of wavelet parameters in the performance of WANN drought forecasting models in Algeria.

Drought was forecasted for various lead times varying from 1-month to the maximum forecast lead time in the Algerois catchment by taking into account the SPI as a drought measurement indicator.

2 Methodology

2.1 The Standardized Precipitation Index (SPI)

The SPI was developed by McKee et al. (1993) and it quantifies drought also in the present study due to the following advantages.

Its calculation needs only precipitation data; it can be calculated for any time scale; and the frequency of extreme and severe droughts is consistent (Hayes et al. 1999; WMO, 2012). Even during the winter season, the SPI is just as effective and does not depnd on topographical features. The SPI computation is based on the long-term monthly precipitation record (McKee et al. 1993) fitted to gamma distribution, transformed thereafter to the standard normal random variable Z, which is the value of the SPI (Edwards and McKee 1997).

2.2 Artificial Neural Networks (ANN)

ANNs are nonlinear models that can learn patterns from data in adaptive manner. The feedforward model is the most frequently utilized for time series forecasting among the various types of ANN models. It is constituted of many layers of neurons, where external informa-

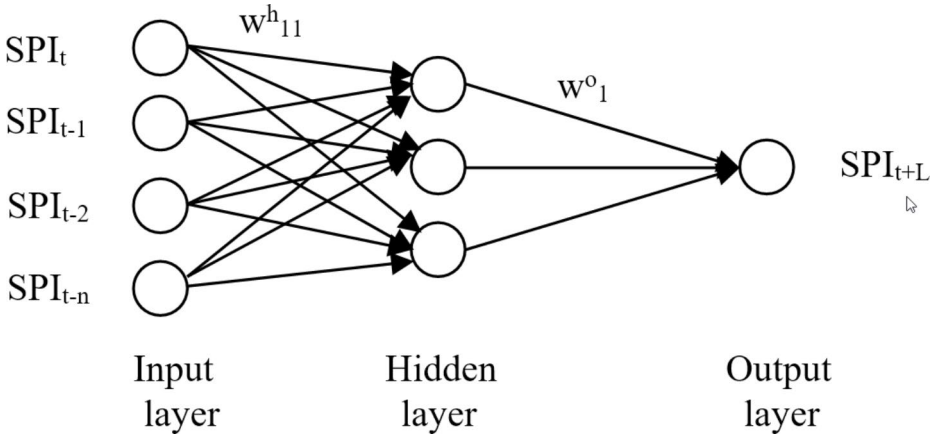

Fig. 1 The proposed Feed-forward Neural network

tion is received by the input layer while output layer consists of forecast results. The input and output layers are separated by.

one or more hidden layers as in the proposed ANN model in Fig. 1.

ANN application basically consists of three steps: network architecture definition, network training, and network testing. One of the most commonly-used algorithms for ANN training is the Levenberg Marquardt (LM) back propagation algorithm (Noori et al. 2011), which is also applied in the present work.

2.3 Wavelet Artificial Neural Networks (WANN)

WANN is an abbreviation for the combination of wavelet decomposition and ANN. Inputs are decomposed by wavelet into approximations and details components.

2.3.1 Wavelet Decomposition

Wavelet decomposition is suitable to study non-stationary times series. It can reveal aspects of data such as trends, breakdown points, and discontinuities that other tools may overlook. (Kim and Valdes 2003).

For a time series, f(t), the continuous wavelet transform (CWT) at time t is defined by: (Shoaib et al. 2014) as follows.

$$W_{a,b}(t) = \int_{-\infty}^{+\infty} f(t) \frac{1}{\sqrt{a}} \psi^{*}\left(\frac{t-b}{a}\right) dt \tag{1}$$

where :

*: complex conjugate of the function.

a: dilation (scale) parameter.

b: translation (position) parameter.

CWT is characterized by redundancy and as a substitute Discrete Wavelet Transform (DWT) is used (Maheswaran and Khosa 2012), the expression of which is given below.

.

$$W(a,b)_D = 2^{-j/2} \int_{j=1}^{j=J} \psi^* \left(2^{-j/2} - k \right) f(t)\, dt \tag{2}$$

where, k, j: integers that control the wavelet translation and dilation. The a' trous algorithm is used. Corresponding to the original series x(t), smoother versions of x(t) are defined at different scales as given by the following equations.

$$c_0(t) = x(t) \tag{3}$$

$$c_j(t) = \sum_{l=-\infty}^{\infty} h(l)\, c_j\left(t + 2^{j-1} l\right) \tag{4}$$

where j is the level of decomposition and h(l) is a low pass filter with compact support.

The detail component of *x(t)* at level i is defined as,

$$d_j(t) = c_{j-1}(t) - c_j(t) \tag{5}$$

The set $\{d_1, d_2, \ldots, d_p, c_p\}$ in this last expression represents the additive wavelet decompositions of the data up to resolution level p and c_p is the residual component.

The choice of the best mother wavelet and decomposition level are of utmost importance (Nourani et al. 2014). Many of hydrological studies regarding the performance of different mother wavelets have concluded that the appropriate mother wavelet is ideally determined by a trial-and-error process (Maheswaran and Khosa 2012; Nalley et al. 2012; Nourani et al. 2011; Sang 2012).

2.3.2 Selection of Wavelet Families

The best mother wavelet function choice is difficult and influenced by the time series at hand as well as some of properties of the wavelet functions (Maheswaran and Khosa 2012). The present study compares the effects of 39 selected wavelet functions on the performance of hybrid Wavelet-ANN (WANN) models. Below, is an overview of the used wavelet families, and more details can be found in many standard text books such Daubechies (1992), Addison (2002) and Walker (2008).

Haar Wavelet It was proposed by Haar (1910) as the simplest mother wavelet because it has just two scaling coefficients both of which are equal to one, but non-continuous, symmetric and have one vanishing moments.

Daubechies Wavelets It has a compact support, highest number of vanishing moments and extreme phase. They have minimum phase associative scaling filters and are orthogonal and bi-orthogonal. Daubechies wavelets are very good at capturing polynomial behaviour in

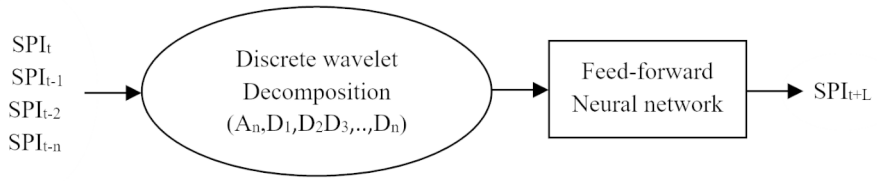

Fig. 2 Schematic diagram of the proposed WANN model

signals. It is denoted by dbN, where N is the number of vanishing moments (in this study N is varied between 2 and 17).

Symmlets Daubechies wavelets are quite symmetric, so it is important to improve symmetry while retaining simplicity, Daubechies proposed Symmlets as a modification to her original wavelets (also spelled symlets) (Addison 2002). They have $N_k/2-1$ vanishing moments, support length N_k-1 and filter length N_k. In this study, we used 16 members of this wavelet family, namely the Sym2, Sym3, …, Sym17.

Coi *flets*: Coiflets are another wavelet family found by Daubechies. They are also nearly symmetrical and have vanishing moments. It has only five members from Coif1 with 1 to Coif5 with 5.

Meyer Wavelet Constructed by Meyer (1985), It's the second orthogonal wavelet. To define the Meyer wavelet function and the corresponding scaling functions, the frequency domain is used (Meyer 1992).

2.3.3 Hybrid wavelet-ANN Model Development

WANN models are constructed taking into account the discrete wavelets of SPI time series as inputs to the ANN and the original SPI time series as outputs, which lead to the hybrid Wavelet-ANN models (WANN). The 39 selected mother wavelet functions are used to divide the original SPI series into approximations and details in order to investigate the effect of DWT pre-processing on the effectiveness of ANN models for long lead time drought forecasting. Figure 2 illustrates the proposed WANN model.

2.4 Performance Measures

The following goodness of fit measures were used to evaluate the forecast performance of all proposed models.

Nash-Sutcliffe Efficiency Coefficient (NSE) It is sensitive to additive and proportional differences between forecasts and observations (Legates and McCabe 1999).

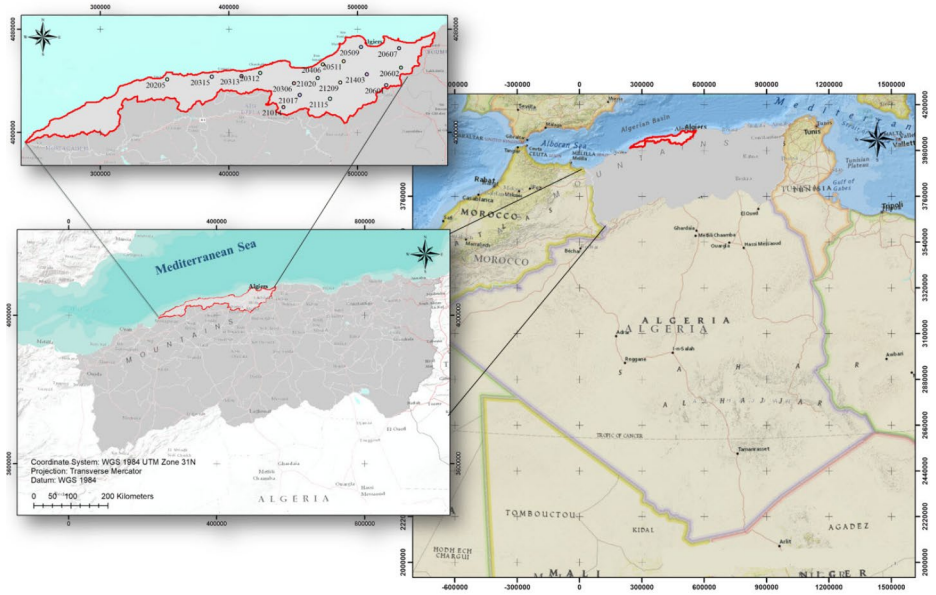

Fig. 3 Location of rain gauge stations used in the study

$$NSE = 1 - \frac{\Sigma_{i=1}^{N}(SPI_i - \widehat{SPI_i})^2}{\Sigma_{i=1}^{N}(SPI_i - \overline{SPI})^2} \tag{6}$$

Root Mean Squared Error *and* **Mean Absolute Error** They describe the difference in observed and forecasted values as well accepted absolute indicators for continuous variables (Legates and McCabe 1999). They are given by.

$$RMSE = \sqrt{\frac{\sum_{i=1}^{N}(SPI_i - \widehat{SPI_i})^2}{N}} \tag{7}$$

$$MAE = \frac{\sum_{i=1}^{N}\left|SPI_i - \widehat{SPI_i}\right|}{N} \tag{8}$$

2.5 Study area and Database

The study area is located in the western part of the Algerois watershed (Fig. 3) it covers 5,225.3 km^2. It has a Mediterranean climate with average annual rainfall of 600 to 800 mm in the coastal regions and 500 to 1,000 mm in the interior.

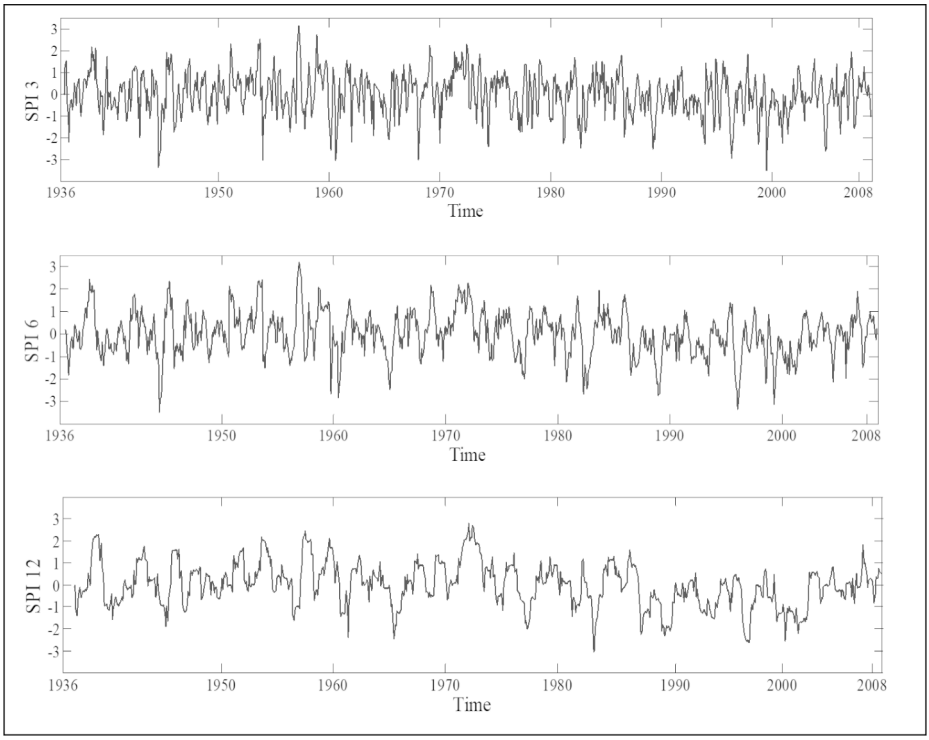

Fig. 4 SPIs time series

In order to estimate the mean areal rainfall, the Thiessen polygon method is used for historical monthly rainfall data from the year 1936 to 2008 available at 17 rainfall gauging stations.

3 Results and Discussions

Theissen polygon method estimates average areal precipitation, which was used to calculate SPI time series. The SPI series of three-, six- and twelve-month time scales are shown in Fig. 4.

3.1 ANN Models

Optimal ANN models for SPI series are identified by trial-and-error approach. The number of tested input neurons ranged from 1 to 20. The number of hidden nodes was gradually increased from 1 to 20 for each input layer dimension. The combination with the best performance measures is selected. The early stopping technique is used in this work to prevent overfitting. NSE, RMSE and MAE for each combination are calculated.

NSE for different ANN combination for SPI-12, is presented in Fig. 5. It has been noticed that there is no improvement from 13 input neurons onwards. So, ANN model with 13 and

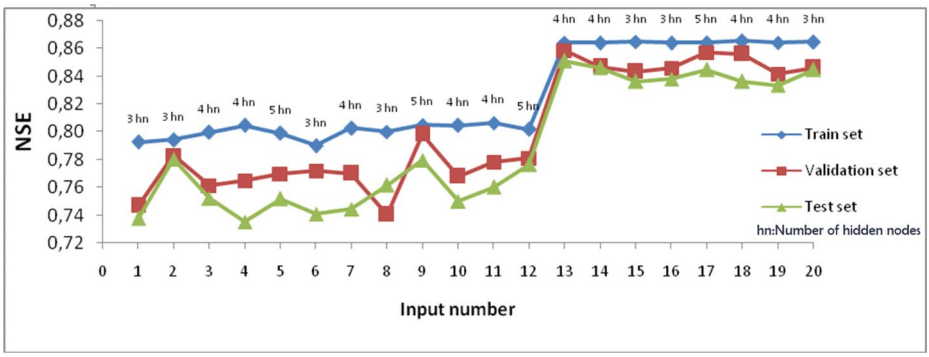

Fig. 5 NSE Evolution for different input number

Table 1 ANN forecasts

Lead- time (month)	NSE	RMSE	MAE	ANN Structure
	(a) SPI-3			
1	0.4499	0.7255	0.579	4-10-1
2	0.1619	0.8905	0.6959	4-11-1
3	-0.0028	0.9754	0.7548	4-13-1
4	-0.008	0.9787	0.76	4-15-1
5	-0.0094	0.9818	0.7657	4-18-1
6	-0.0343	0.9906	0.7766	4-20-1
	(b) SPI-6			
1	0.7056	0.5111	0.4043	7-4-1
2	0.4706	0.6873	0.5479	7-5-1
3	0.2831	0.7976	0.6642	7-7-1
4	0.1241	0.8817	0.7048	7-8-1
5	0.0240	0.9307	0.7209	7-10-1
6	-0.0959	0.9888	0.7578	7-11-1
	(c) SPI-12			
1	0.8608	0.3252	0.2422	13-4-1
2	0.7040	0.4743	0.3590	13-4-1
3	0.5805	0.5646	0.4112	13-5-1
4	0.4200	0.6639	0.5007	13-6-1
5	0.3106	0.7238	0.5749	13-6-1
6	0.2095	0.7751	0.6118	13-7-1

4 neurons in the input and the hidden layers respectively is are chosen as a drought forecasting model for the SPI-12. Similarly, the optimal models for the other SPIs series results are given in Table 1.

In this study, the autocorrelation function (ACF) and the partial autocorrelation function (PACF) are employed to confirm the number of inputs corresponding to different antecedents values.

Figure 6 presents these functions for SPI-12. It is clear that the ACF has a peak at lag 12. As a result, twelve antecedent SPI values contain the most information for predicting future droughts, which are used as input for ANN models. The same results are obtained for 3- and 6- month SPI, which ACF functions exhibit peaks at lags 3 and 6, respectively.

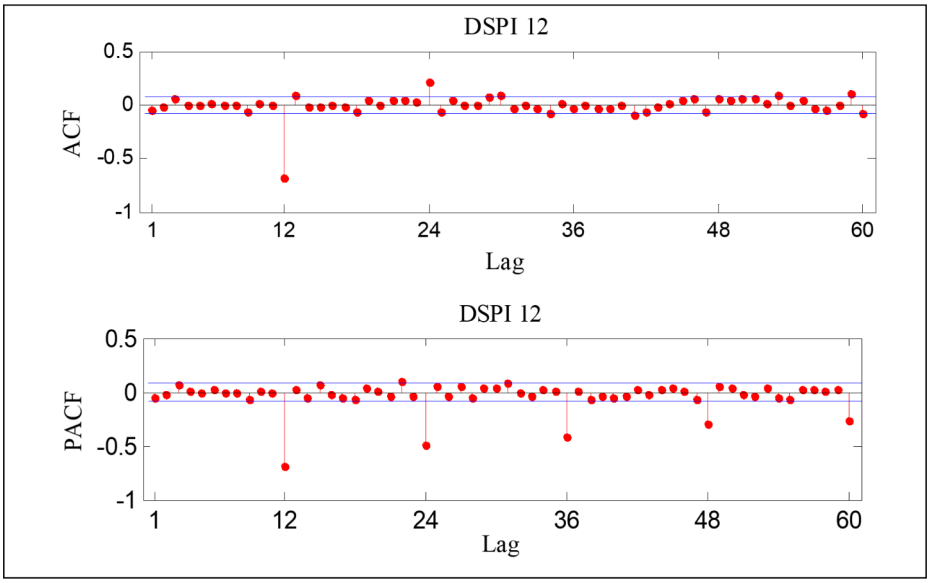

Fig. 6 SPI-12 series ACF and PACF

The best ANN model structures are used to forecast droughts at different lead times and the results are shown in Table 1.

3.2 WANN Models

The purpose of this research is to look into the effects of different wavelet families and the decomposition level on the performance of WANN models. For this reason, a two-step procedure applies as follows.

i. The selection for each wavelet family of the appropriate vanishing moment number, and the corresponding optimum level of decomposition level for all SPIs time scales are used for all forecast lead time.
ii. Comparison between the efficient wavelet function selections among the 39 are used as mother wavelet.

For this reason, the performance of hybrid WANN models is examined for the 39 selected wavelet function derived from 5 wavelet families, including Haar(db1), Daubechies (from db2 to db17), Symlets (from Sym2 to Sym17), Coiflets (from Coif1 to coif5) and the Discrete approximation of Meyer (dmey).

SPI time series is decomposed between 1 and 6 levels using the 39 selected discrete wavelet functions to determine the appropriate wavelet function and the optimum decomposition level.

Once SPI time series are successfully decomposed, these coefficients of details and approximations are used as input to ANN component of the hybrid model WANN to obtain the output prediction. Following the decomposition of SPI time series, the obtained coef-

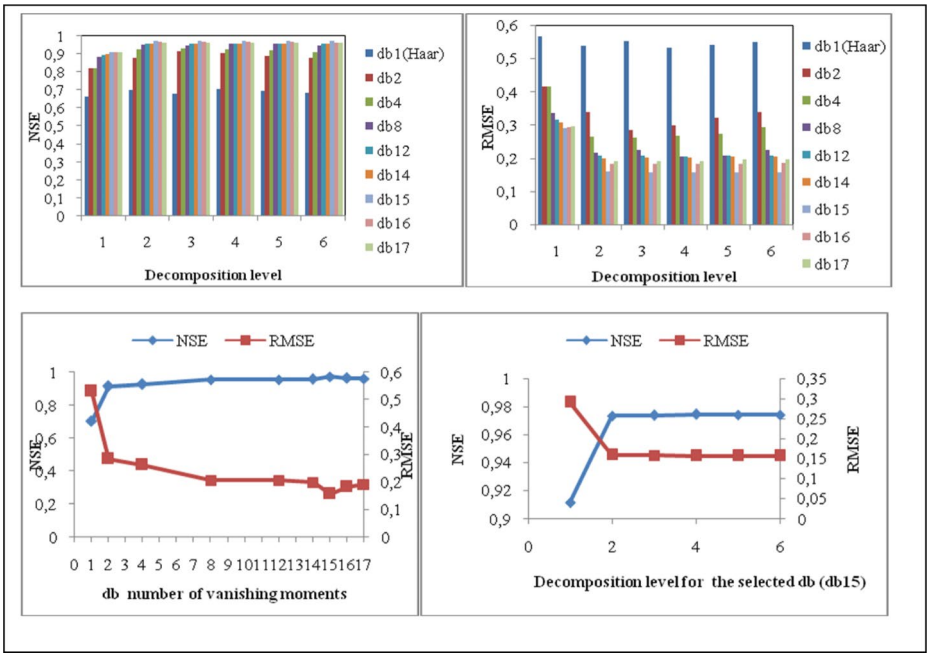

Fig. 7 Effect of vanishing moments and decomposition level in db wavelet family on NSE and RMSE (SPI-3, 1-month lead time)

ficients of details and approximations are considered as input to the ANN model to obtain the output prediction. Optimal WANN architecture is reached by trial-and-error approach.

As we cannot display all results in this paper, we will just present some illustrative result of the SPI-3 series for1-month lead forecast.

Starting with Daubechies wavelet family, to determine the best wavelet mother function, the vanishing moments number is varied from 1 (Haar) to 17. For each vanishing moment number, the SPI time series is decomposed up to 6th level in order to determine the optimum decomposition level.

The effect of the vanishing moment number and the decomposition level in db wavelet family is shown in Fig. 7, which shows that db15 (15 vanishing moment) is the most well adapted function at the fourth decomposition level.

From the results, it can be deduced that the WANN model with the db15 wavelet function is better than the other 17 models. Daubechies wavelets being tested with NSE equal to 0.9745 and lowest RMSE and MAE values are 0.1563, 0.1224, respectively.

The same strategy was adopted for Symlets and Coiflets wavelet families. For Symlets, to determine the best wavelet mother function the vanishing moments number is varied from 2 to 17. For each vanishing moment number, the SPI time series are decomposed up to 6th level in order to determine the optimum level of decomposition. The forecast results indicate that Sym15 is the best Symlets function at the fourth decomposition level. The results are shown in Table 2.

For the Coiflets family, the forecast results indicate that Coif5 is the best Coiflets Symlets function at the second decomposition level. The results are given also in Table 2.

Table 2 Decomposition level effect on discrete Meyer (dmey) performance (SPI-3, 1-month lead time forecast)

Mother wavelet	Forecasting Measures	Decomposition levels						Optimum level
		1	2	3	4	5	6	
Dmey	NSE	0.9307	0.9749	0.9755	***0.9758***	0.9754	0.9753	4
	RMSE	0.2575	0.1549	0.1532	***0.1523***	0.1535	0.1538	
	MAE	0.1987	0.1247	0.1227	***0.1224***	0.1217	0.1230	

Table 3 WANN forecasts for SPI-3

Selected Mother wavelet	Lead- time (month)	Optimum decomposition level	NSE	RMSE	MAE	WANN Structure
Discrete Meyer (dmey)	1	4	0.9758	0.1523	0.1224	20-2-1
	3	3	0.8438	0.3866	0.3081	16-2-1
	6	4	0.5904	0.6260	0.5012	20-2-1
	7	4	0.5375	0.6653	0.5260	20-3-1
	8	4	0.3932	0.7620	0.5863	20-3-1
Daubechies(db15)	1	4	0.9745	0.1563	0.1262	20-2-1
	3	4	0.8376	0.3970	0.3064	20-2-1
	6	4	0.6920	0.5429	0.4292	20-2-1
	7	4	0.6097	0.6111	0.4938	20-3-1
	8	4	0.4852	0.7019	0.5614	20-3-1
Symlets(Sym15)	1	3	0.9693	0.1715	0.1276	16-2-1
	3	4	0.8260	0.4080	0.3139	20-2-1
	6	4	0.6918	0.5400	0.4282	20-2-1
	7	4	0.5787	0.6349	0.5098	20-3-1
	8	4	0.4611	0.7181	0.5844	20-3-1
Coiflets(Coif5)	1	2	0.9538	0.2102	0.1657	12-2-1
	3	4	0.7950	0.4429	0.3569	20-2-1
	6	4	0.5615	0.6441	0.4882	20-2-1
	7	4	0.4530	0.7194	0.5492	20-3-1
	8	4	0.3103	0.8078	0.6108	20-3-1

Finally, the discrete approximation of Meyer (dmey) wavelet family has one mother function. In this case only, the decomposition level is varied from 1 to 6 in order to determine the optimum decomposition level. The forecast results of SPI-3, presented in Table 3, show that discrete Meyer (dmey) wavelet mother with an optimum decomposition level of 4 have the best performance with NSE equal to 0.9758, RMSE and MAE equal to 0.1523,0.1224, respectively.

For the other lead times, the vanishing moments number is fixed based on the 1-month lead time forecasts, but the decomposition level is varied from 1 to 6. The results are presented in Table 2.

Following the same approach for SPI-6 and SPI-12 series, the results show that the best wavelet mother functions for SPI-6 are db13, Sym13, Coif5 and dmey, and for SPI-12 series the best wavelet mother functions are db13, Sym14, Coif5 and dmey.

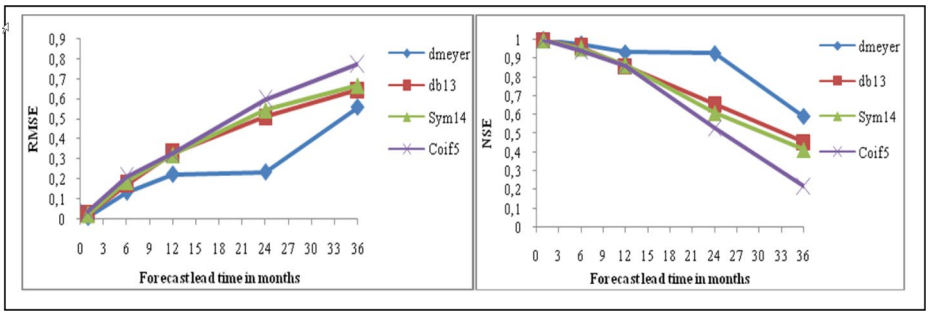

Fig. 8 Evolution of NSE and RMSE over different forecast lead time for SPI-12

3.3 Evaluation of Models' Performance

The purpose of this research is to look into the effects of various wavelets families and the decomposition level on the performance of the proposed drought forecasting models for long lead time. For this purpose, taking the optimal ANN and WANN models, time series of the SPI for the three-time scales (3-, 6- and 12-month) are forecasted for the maximum lead time (we consider accepted efficiency for NSE≥0.50). The results are presented in Tables 3, 4 and 5.

The results show that, for ANN and WANN models, the forecast accuracy is lower in SPI-3, but the best forecasts are those of SPI-12, which is caused by the high temporal rainfall variability in SPI-3, whereas this variability is reduced in the other scales, due to the fact that more monthly data is summed. Hence, the forecast accuracy is proportional to the SPI time scale. When the forecast lead time is risen, an important increase appears in the RMSE and a significant decrease in the NSE occurs for all models, which is very frequent in forecasting models.

The results of the ANN without wavelet transformation are shown in Table 1. For 1-month lead forecast, SPI-3, SPI-6 and SPI-12 results are satisfactory. For 2- and 3-months lead times, only SPI-12 forecasts are acceptable. The drought's evolution cannot be represented by ANN.

For the WANN models, as indicated earlier for 1-month lead time forecast, the three SPI time series are decomposed between 1 and 6 levels using the 39 selected discrete wavelet function, and thus a total of 702 WANN models are analyzed. Thereafter, for the other lead times only the decomposition level is varied up 6th level for the four selected wavelet functions, which add to 288 models to the latter, so a total of 990 WANN models are analysed in the present study. Figure 8 shows an example of the evolution of NSE and RMSE for different lead time forecast for the SPI-12.

The maximum decomposition level of discrete wavelet transforms is calclulated generally using the following equation : $L = int\left[\log\left(N\right)\right]$, where L is the level and N the total data number. On the basis of this equation with N equal to 874, 871 and 865 for the the SPI-3, SPI-6 and SPI-12 respectively correspond to L value is 2.

However, in this study it is found that the optimum decomposition level depends on three parameters, namely, the wavelet function; for example, for SPI-3 series (1-month lead time forecast) the optimum decomposition level for the wavelet mother dmey, db15, Sym15 and Coif5, equal to 4, 4, 3 and 2 respectively. On the forecast lead time, as it is indicated by the

Table 4 WANN forecasts for SPI-6

Selected Mother wavelet	Lead- time (month)	Optimum decomposition level	NSE	RMSE	MAE	WANN Structure
Discrete Meyer(dmey)	1	2	0.9967	0.0543	0.0406	21-2-1
	3	3	0.9462	0.2185	0.1644	28-2-1
	6	3	0.8809	0.3252	0.2664	28-2-1
	12	5	0.6742	0.5377	0.4239	42-2-1
	18	5	0.5029	0.6642	0.5076	42-2-1
Daubechies(db13)	1	4	0.9948	0.0676	0.0522	35-2-1
	3	4	0.9118	0.2797	0.2184	35-2-1
	6	4	0.8166	0.4034	0.3152	35-2-1
	12	5	0.5631	0.6227	0.4754	42-2-1
	18	5	0.2800	0.7994	0.6174	42-2-1
Symlets(db13)	1	4	0.9945	0.0700	0.0529	35-2-1
	3	3	0.9129	0.2780	0.2140	28-2-1
	6	4	0.8588	0.3540	0.2778	35-2-1
	12	5	0.6313	0.5720	0.4422	42-2-1
	18	5	0.3986	0.7305	0.5594	42-2-1
Coiflets(Coif5)	1	4	0.9937	0.0747	0.0570	35-2-1
	3	3	0.8968	0.3026	0.2364	28-2-1
	6	4	0.8128	0.4076	0.3225	35-2-1
	12	5	0.5019	0.6649	0.5193	42-2-1
	18	5	0.1359	0.8757	0.6826	42-2-1

results of SPI-12 series, for example for dmey the optimum decomposition level equal to 2 and 5 for the 1-month and the 36-month lead forecasts, respectively. Finally, on time series complexity, for example for 1-month lead forecast using dmey wavelet function, the 2nd decomposition level is sufficient to capture the variation of the SPI-12 series, while, for the SPI-3 decomposition up to 4th level is needed. These results confirm the limitation of the formula evoked by Nourani et al. (2011). Stating that this formula is based on fully autoregressive times series, it only takes into account the length of the time series and ignores seasonal effects.

The results of the best selected WANN models with maximum lead time forecasts are displayed in Tables 2, 4 and 5. The use of wavelets transforms gives more accurate forecasting models. Compared to ANN models, WANN results show a higher NSE values, but lower RMSE and MAE values.

Furthermore, as compared to ANN models, the number of hidden nodes decreases, this is due to the fact that wavelet decomposition reduces time series complexity.

For the SPI-3 series, from Table 2, it can be shown that maximum forecast lead time is 7-months, which is obtained with all the selected mother wavelet except the coif5. The best wavelet mother for 1-month and 3-month lead time are the dmey followed by db15 and sym15, which provide comparable results, and then the Coif5. For 6-month and 7-month lead time forecasts appear as the best results of db15 and sym15 is followed by dmey, and then the Coif5, which shows the poor forecast results. For the maximum forecast lead time (7-month) the best results were obtained by db15 with NSE equal to 0.6097 and lowest RMSE and MAE equal to 0.6111, 0.4938, respectively. SPI-3 forecasts for 1-month and 7-month lead time are shown in Fig. 9 and Fig. 10.

Table 5 WANN models forecasts for SPI-12

Selected Mother wavelet	Lead- time (month)	Optimum decomposition level	NSE	RMSE	MAE	WANN Structure
Discrete Meyer(dmey)	1	2	0.9999	0.0080	0.0062	39-2-1
	6	4	0.9767	0.1330	0.1009	65-2-1
	12	4	0.9344	0.2232	0.1745	65-2-1
	24	4	0.9276	0.2346	0.1808	65-2-1
	36	5	0.5916	0.5571	0.4511	78-2-1
Daubechies(db13)	1	2	0.9994	0.0215	0.0167	39-2-1
	6	4	0.9607	0.1732	0.1377	65-2-1
	12	5	0.8586	0.3278	0.2524	78-2-1
	24	5	0.6559	0.5113	0.3925	78-2-1
	36	5	0.4548	0.6437	0.5035	78-2-1
Symlets(Sym14)	1	3	0.9994	0.0222	0.0173	52-2-1
	6	4	0.9537	0.1876	0.1391	65-2-1
	12	5	0.8639	0.3216	0.2426	78-2-1
	24	5	0.6105	0.5440	0.4345	78-2-1
	36	5	0.4142	0.6672	0.5306	78-2-1
Coiflets(Coif5)	1	4	0.9983	0.0356	0.0275	65-2-1
	6	4	0.9407	0.2127	0.1693	65-2-1
	12	4	0.8588	0.3276	0.2528	65-2-1
	24	5	0.5292	0.5981	0.4534	78-2-1
	36	5	0.2161	0.7718	0.6123	78-2-1

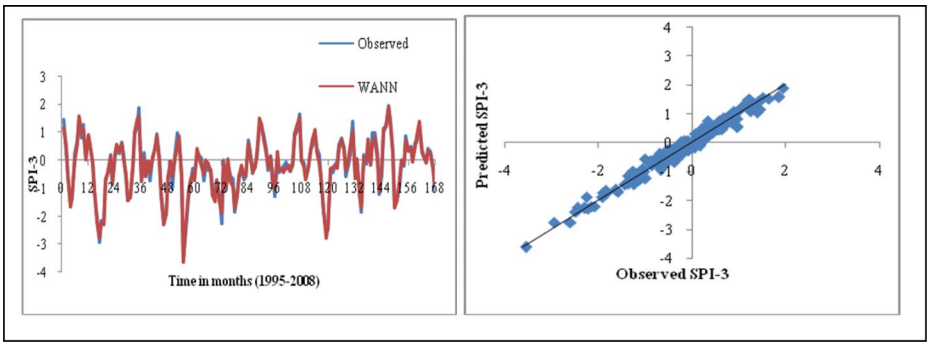

Fig. 9 SPI-3 forecasts for 1-months lead time

For the SPI-6, it has been found that the performance of the dmey is the best for all forecast lead times, followed by db13 and sym13, which have closer results, and then the Coif5. The maximum forecast lead time is 18-months obtained only by the dmey mother wavelet with NSE equal to 0.5029 and lowest RMSE and MAE equal to 0.6642, 0.5076, respectively. SPI-6 for 18-months lead forecasts is shown in Fig. 11.

The performance of the dmey for the SPI-12, has been found as the best for all forecast lead times, followed by db13 and sym14, which have closer results, and then the Coif5. The maximum forecast lead time is 36-months obtained only by the dmey mother wavelet with NSE equal to 0.5916 and lowest RMSE and MAE equal to 0.5571, 0.4511, respectively.

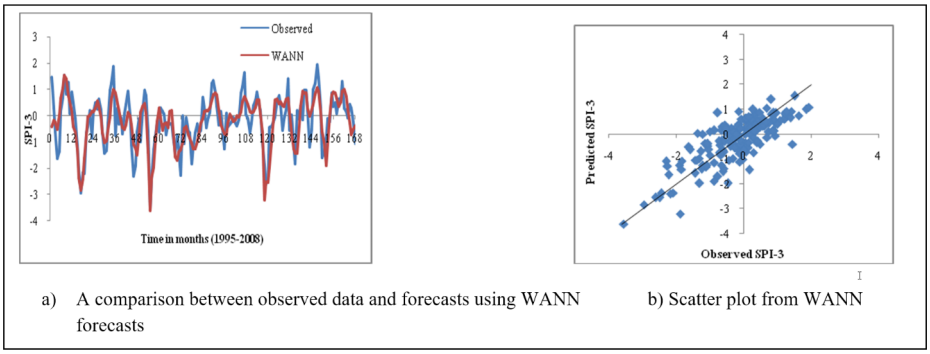

a) A comparison between observed data and forecasts using WANN forecasts

b) Scatter plot from WANN

Fig. 10 SPI-3 forecasts for 7-months lead time (maximum forecast lead time)

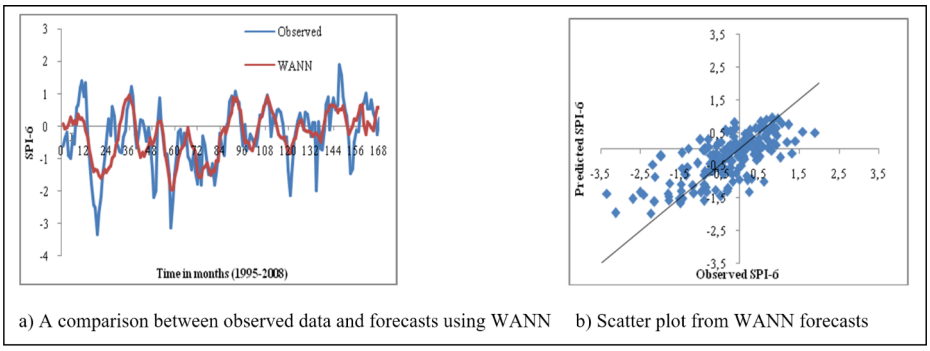

a) A comparison between observed data and forecasts using WANN

b) Scatter plot from WANN forecasts

Fig. 11 SPI-6 forecasts for 18-months lead time (maximum forecast lead time)

SPI-12 for 36-month lead forecasts is shown in Fig. 12. The figure shows that there is no significant overestimation or underestimating, and the points are near to the trend line.

From the results, it can be seen that the WANN models are strongly performed than the ANN models. Also, as the forecast lead time increased, the forecast performance for all models decreased.

Daubechies and Symlets wavelet families have similar vanishing moments number and optimum decomposition levels, this is due to fact that their constructions are very similar.

SPI times series are complex, for this reason a higher vanishing moments number is needed to capture information from the SPI time series. This can be explained by the fact that more vanishing moments indicate that scaling function can accurately represent more complicated signals.

4 Conclusion

This study searches for the effect of different mother wavelets and the decomposition level on the performance of the hybrid discrete WANN drought forecasting models.

To quantify drought the standard precipitation index (SPI) is selected as a drought indictor the in the Algerois catchement in North Algeria. The SPI was chosen, due to its multiple

a) A comparison between observed data and forecasts using WANN b) Scatter plot from WANN forecasts

Fig. 12 SPI-12 forecasts for 36-months lead time (maximum forecast lead time)

advantages compared to other drought indices. Using SPI leads to most sorts of drought episodes quantification. The SPI time scales represent how drought affects the availability of various water resources. For this reason SPI-3 is used, which reflects short and medium term moisture conditions, SPI-6 can be related with anomalous stream flows and reservoir levels, and finally, SPI-12 provides reflection of long-term rainfall patterns and they are usually tied to groundwater levels, stream flows and reservoir levels (WMO, 2012).

The best models are employed forecast droughts for various lead times varying from 1-month to the maximum forecast lead time possible. Comparison and evaluation of forecasting models are based on best performance measures.

Wavelet decomposition improves ANN model performance by taking useful information at multiple resolution levels. It also minimizes the time series complexity, consequently the number of hidden nodes. The WANN models with Meyer discrete approximation have the best forecast performance.

The optimum decomposition level depends on three parameters, which are the wavelet function, the time series complexity and the forecast lead time. Also, the vanishing moment number depends on the time series complexity.

The maximum forecast lead times reached (we consider accepted efficiency for NSE ≥ 0.50) are 36-month for SPI-12, 18-month for SPI-6 and 7- month for the SPI-3.

The developed WANN models can be used in other Algerian basins to develop effective water resources management and monitoring. This study focused on the effect of the wavelet transform on the performance of hybrid wavelet neural network models. For future studies, it is recommended to evaluate the effect of the wavelet transform on the performance of other hybrid wavelet artificial intelligence-based models. It is also recommended to investigate this approach in different climatic regions.

Author Contributions All authors contributed to the study conception and design. Material preparation, data collection and analysis were performed by [Djerbouai Salim], [Souag-Gamane Doudja] and [Djoukbala Omar]. The first draft of the manuscript was written by [Djerbouai Salim], [Souag-Gamane Doudja], [Hasbaia Mahmoud] and all authors commented on previous versions of the manuscript. review and editing by [Ferhati Ahmed], [Benselama Oussama] and [Dougha Mostafa]. All authors read and approved the final manuscript.

Funding The authors declare that no funds, grants, or other support were received during the preparation of this manuscript.

Data Availability is decomposed into three parts. First 60% i were allocated for model training, the next 20% for model validation, and the resting 20% for testing the model.

Data Availability The authors confirm that all data and materials as well as software applications or custom code support their published claims and conform to field standards.

Declarations

Ethical Approval This paper has neither been published nor been under review for publication elsewhere.

Consent to Participate The authors have participated in the preparation and submission of this paper for publication in the Water Resources Management.

Consent to Publish The authors would like to publish their paper in Water Resources Management.

Competing Interests The authors have no relevant financial or non-financial interests to disclose, and they have no conflicts of interest to declare that are relevant to the content of this paper and its publication.

References

Addison PS (2002) The Illustrated Wavelet transform handbook: introductory theory and applications in Science, Engineering, Medicine and Finance, 1st edn. CRC Press. https://doi.org/10.1201/9781003040408

Aghelpour P, Bahrami-Pichaghchi H, VarshavianV (2021) Hydrological drought forecasting using multiscalar streamflow drought index, stochastic models and machine learning approaches, in northern Iran. Stoch Environ Res Risk Assess. https://doi.org/10.1007/s00477-020-01949-z

Anshuka A, van Ogtrop FF, Willem Vervoort R (2019) Drought forecasting through statistical models using standardised precipitation index: a systematic review and meta-regression analysis. Nat Hazards 97:955977. https://doi.org/10.1007/s11069-019-03665-6

Barua S, Ng AWM, Perera BJC (2012) Artificial neural network-based drought forecasting using a nonlinear aggregated drought index. J Hydrol Eng 17:1408–1413. doi:https://doi.org/10.1061/ASCE

Belayneh A, Adamowski J (2012) Standard Precipitation Index drought forecasting using neural networks, wavelet neural networks, and support vector regression. Appl Comput Intell Soft Comput Article ID 794061:13pages. https://doi.org/10.1155/2012/794061

Belayneh A, Adamowski J, Khalil B, Ozga-Zielinski B (2014) Long-term SPI drought forecasting in the Awash River Basin in Ethiopia using wavelet neural networks and wavelet support vector regression models. J Hydrol 508:418–429. https://doi.org/10.1016/j.jhydrol.2013.10.052

Belayneh A, Adamowski J, Khalil B, Quilty J (2014) Coupling machine learning methods with wavelet transforms and the bootstrap and boosting ensemble approaches for drought prediction. Atmos Res 172–173:37–47. https://doi.org/10.1016/j.atmosres

Bordi I, Sutera A (2007) Drought monitoring and forecasting at large scale. In: Rossi G, Vega T, Bonaccorso B (eds) Methods and tools for Drought Analysis and Management. Springer, Dordrecht,pp, pp 3–27

Daubechies I (1992) Ten lectures on wavelets. Society for Industrial & Applied Mathematics. ISBN: 978-0 89871-274-2

Djerbouai S, Souag-Gamane D (2016) Drought forecasting using neural networks, wavelet neural networks, and stochastic models: case of the Algerois Basin in North Algeria. Water Resour Manage 30:2445–2464. doi:https://doi.org/10.1007/s11269-016-1298-6

Drisya J, Kumar DS, Roshni T (2021) Hydrological drought assessment through streamflow forecasting using wavelet enabled artificial neural networks. Environ Dev Sustain 23:3653–3672. https://doi.org/10.1007/s10668-020-00737-7

Edwards DC, McKee TB (1997) Characteristics of 20th century drought in the United States at multiple time scales. Colorado State University, Fort Collins. Climatology Report No. 97 – 2, CO, USA

Fernández C, Vega JA, Fonturbel T, Jiménez E (2009) Streamflow drought time series forecasting: a case study in a small watershed in North West Spain. Stoch Env Res Risk Assess 23:1063–1070. https://doi.org/10.1007/s00477-008-0277-8

Hayes MJ, Svoboda MD, Wilhite DA, Vanyarkho OV (1999) Monitoring the 1996 drought using the standardized precipitation index. Bull Am Meteorol Soc 80:429–438. https://doi.org/10.1111/j.1752-1688.1999.tb03592.x

Hayes M, Svoboda M, Wall N, Widhalm M (2011) The Lincoln Declaration on Drought Indices: Universal Meteorological Drought Index recommended. Bull Am Meteorol Soc 92(4):485–488 Retrieved Dec 27, 2022, from. https://journals.ametsoc.org/view/journals/bams/92/4/2010bams3103_1.xml

Han P, Wang PX, Zhang SY, Zhu DH (2010) Drought forecasting based on the remote sensing data using ARIMA Models. Math Comput Model 51(11–12):1398–1403. https://doi.org/10.1016/j.mcm.2009.10.031

Han P, Wang P, Tian M, Zhang S, Liu J, Zhu D (2013) Application of the ARIMA models in drought forecasting using the standardized precipitation index. IFIP Adv Inform Communication Technol 352–358. doi:https://doi.org/10.1007/978-3-642-36124-1_42

Hosseini-Moghari SM, Araghinejad S (2015) Monthly and seasonal drought forecasting using statistical neural networks. Environ Earth Sci 74:397–412. doi:https://doi.org/10.1007/s12665-015-4047-x

Jalalkamali A, Moradi M, Moradi N (2015) Application of several artificial intelligence models and ARIMAX model for forecasting drought using the standardized precipitation index. Int J Environ Sci Technol 12:1201–1210. https://doi.org/10.1007/s13762-014-0717

Karthika M, Krishnaveni M, Thirunavukkarasu V (2017) Forecasting of meteorological drought using ARIMA model. Indian J Agricultural Res 51:103–111. doi:https://doi.org/10.18805/ijare.v0iOF.7631

Kim T, Valdes JB (2003) Nonlinear model for drought forecasting based on a conjunction of wavelet transforms and neural networks. Hydrologic Eng 8:319–328. https://doi.org/10.1061/(ASCE)10840699(2003)8:6(319)

Kousari MR, Hosseini ME, Ahani H, Hakimelahi H (2017) Introducing an operational method to forecast long-term regional drought based on the application of artificial intelligence capabilities. Theoret Appl Climatol 127:361–380. doi:https://doi.org/10.1007/s00704-015-1624-6

Legates DR, McCabe GJ Jr (1999) Evaluating the use of "goodness-of-fit" measures in hydrologic and hydroclimatic model validation. Water Resour Res 35(1):23324. https://doi.org/10.1029/1998WR900018

Maheswaran R, Khosa R (2012) Comparative study of different wavelets for hydrologic forecasting. Comput Geosci 46:284–295. https://doi.org/10.1016/j.cageo.2011.12.015

Marj AF, Meijerink AM (2011) Agricultural drought forecasting using satellite images, climate indices and artificial neural network. Int J Remote Sens 32(24):9707–9719. https://doi.org/10.1080/01431161.2011.575896

McKee TB, Doesken NJ, Kleist J (1993) The Relationship of Drought Frequency and Duration to Time Scales, Paper Presented at 8th Conference on Applied Climatology. American Meteorological Society, Anaheim, CA

Medejerab A, Henia L (2011) Variations spatio-temporelles de la sécheresse climatique en Algérie Nord occidentale. Courrier du savoir 11:71–79

Meyer Y (1992) Wavelet and Applications. Springer

Mishra AK, Desai VR (2005) Drought forecasting using stochastic models. Stoch Env Res Risk Assess 19(5):326–339. https://doi.org/10.1007/s00477-005-0238-4

Mishra AK, Desai VR (2006) Drought forecasting using feed-forward recursive neural network. Ecol Model 198(1–2):127–138. https://doi.org/10.1016/j.ecolmodel.2006.04.017

Mishra AK, Desai VR, Singh VP (2007) Drought forecasting using a hybrid stochastic and neural network model. J Hydrol Eng 12(6):626–638

Modarres R (2007) Streamflow drought time series forecasting. Stoch Env Res Risk Assess 15(21):223–233. https://doi.org/10.1007/s00477-006-0058-1

Morid S, Smakhtin V, Bagherzadeh K (2007) Drought forecasting using artificial neural networks and time series of drought indices. Int J Climatol 27(15):2103–2111. https://doi.org/10.1002/joc.1498

Munir HK, Md SMuhammadN, El-Shafie A (2020) Wavelet Based Hybrid ANN-ARIMA Models for Meteorological Drought forecasting. J Hydrol. doi: https://doi.org/10.1016/j.jhy

Nalley D, Adamowski J, Khalil B (2012) Using discrete wavelet transforms to analyze trends in streamflow and precipitation in Quebec and Ontario (1954–2008). J Hydrol 475(19):204228. https://doi.org/10.1016/j.jhydrol.2012.09.049

Noori R, Karbassi AR, Mehdizadeh H, Vesali-Naseh M, Sabahi MS (2011) A framework development for predicting the longitudinal dispersion coefficient in natural streams using an artificial neural network. Environ Prog Sustain Energy 30(3):439–449

Nourani V, Kisi O, Komasi M (2011) Two hybrid artificial intelligence approaches for modeling rainfall–runoff process. J Hydrol 402(1–2):41–59. https://doi.org/10.1016/j.jhydrol.2011.03.002

Nourani V, Hosseini Baghanam A, Adamowski J, Kisi O (2014) Applications of hybrid wavelet–Artificial Intelligence models in hydrology: a review. J Hydrol 514:358–377. https://doi.org/10.1016/j.jhydrol.2014.03.057

Piri J, Abdolahipour M, Keshtegar B (2022) Advanced Machine Learning Model for Prediction of Drought indices using hybrid SVR-RSM.Water Resources Management1–30
Prasad R, Deo RC, Li Y, Maraseni T (2017) Input selection and performance optimization of ANN-based streamflow forecasts in the drought-prone Murray Darling Basin region using IIS and MODWT algorithm. Atmos Res 197:42–63. doi:https://doi.org/10.1016/j.atmosres.2017.06.014
Roushangar K, Ghasempour R, Nourani V (2022a) Spatiotemporal analysis of droughts over different climate regions using hybrid clustering method. Water Resour Manage 36(2):473–488
Roushangar K, Ghasempour R, Alizadeh F (2022b) Uncertainty Assessment of the Integrated Hybrid Data Processing techniques for short to Long Term Drought forecasting in different climate regions. Water Resour Manage 36(1):273–296
Sang YF (2012) A practical guide to discrete wavelet decomposition of hydrologic time series. Water Resour Manage 26:3345–3365. https://doi.org/10.1007/s11269-012-0075-4
Shirmohammadi B, Moradi H, Moosavi V, Semiromi MT, Zeinali A (2013) Forecasting of meteorological drought using Wavelet-ANFIS hybrid model for different time steps case study: southeastern part of east Azerbaijan province, Iran. Nat Hazards 69:389–402. doi:https://doi.org/10.1007/s11069013-0716-9
Shoaib M, Shamseldin AY, Melville BW (2014) Comparative study of different wavelet based neural network models for rainfall–runoff modeling. J Hydrol 515:47–58. https://doi.org/10.1016/j.jhydrol.2014.04.055
Soh YW, Koo CH, Huang YF, Fung KF (2018) Application of artificial intelligence models for the prediction of standardized precipitation evapotranspiration index (SPEI) at Langat River Basin, Malaysia. Comput Electron Agric 144:164–173. https://doi.org/10.1016/j.compag.2017.12.002
Tigkas D, Vangelis H, Tsakiris G (2019) Drought characterisation based on an agriculture-oriented standardised precipitation index. Theoretical and applied climatology135(3):1435–1447
Walker JS (2008) A primer on Wavelets and their scientific applications. Taylor and Francis group, LLC
Wang Y, Liu J, Li R, Suo X, Lu E (2022) Medium and long-term precipitation prediction using Wavelet decomposition-prediction-reconstruction model. Water Resour Manage 36(3):971–987
Wilhite DA (2000) In: Wilhite DA (ed) Drought as a natural hazard: concepts and definitions. A Global Assessment.Routledge, Drought, pp 3–18
World Meteorological Organization (2012) Standardized precipitation index user guide. World meteorological organization, available at: https://www.droughtmanagement.info/literature/WMO_standardized_precipitation_index_user_guide_en_2012.pdf. Accessed December 27,202
Zhang Y, Yang H, Cui H, Chen Q (2020) Comparison of the ability of ARIMA, WNN and SVM Models for Drought forecasting in the Sanjiang Plain, China. Nat Resour Res 29:1447–1464. https://doi.org/10.1007/s11053-019-09512